A METHODOLOGY FOR THE OPEN LOOP CALIBRATION OF A DEFORMABLE FLAT PLATE ON A 70-METER ANTENNA

David J. Rochblatt[(1)], Daniel J. Hoppe[(1)], William A. Imbriale[(1)], Manuel M. Franco[(1)],

Paul H. Richter[(1)], Phil M. Withington[(2)], Herschel J. Jackson[(1)]

(1) *Jet Propulsion Laboratory*
California Institute of Technology
4800 Oak Grove Drive
Pasadena California 91109
David.j.rochblatt@jpl.nasa.gov

(2) Modern Technologies Corporation
Pasadena, California 91109

INTRODUCTION

This paper describes an experimental study of a deformable flat plate (DFP) Fig. 1, on the NASA-JPL 70-meter antenna (DSS-14) at Ka-Band (32-GHz). The antenna is located at Goldstone California and is part of the NASA-JPL Deep Space Network (DSN). The main purpose of the DFP [1], is to compensate for the gain loss of the 70-meter antenna due to gravity induced structural mechanical deformations to its main reflector surface. At Ka-Band these losses were measured to be 3.6 and 6.5-dB respectively at low and high elevation angles. A novel method for the open loop calibration of a DFP leading to successful gravity compensation over all elevation angles is described. At elevation angles of 10- and 80-degrees, average compensations of 1.7 and 2.3-dB at Ka-Band were achieved.

The open loop calibration of a DFP utilizing 16 actuators was achieved by deriving the gravity deformation of the antenna at all elevation angles from holographic measurements at the three elevation angles of 47.2, 36.7, and 12.7-degrees, and performing a ray trace from the deformed main reflector to the DFP position. The beacons of three geostationary satellite GSTAR-4, GE-2, and INTELSAT 706 were used as far-field signal sources for the three elevation angles respectively at Ku-Band (11-13 GHz). The JPL microwave antenna holography system (MAHST) was used to measure the antenna far-field complex (amplitude and phase) function from which the antenna effective surface deformations were derived [2]. To overcome the difficulty of not having an observable geostationary satellite above 47-degrees elevation, the following assumptions were made in the computation of the surface deformation function:

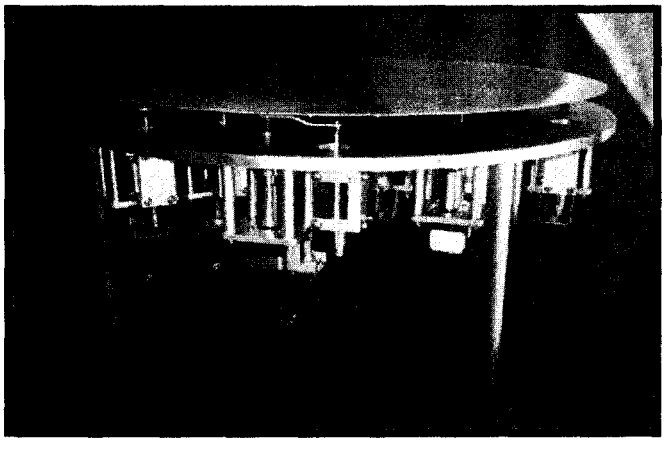

Fig. 1 Deformable Flat Plate

ACKNOWLEDGEMENTS

The work described was funded by the TMOD Technology Program and performed at the Jet Propulsion Laboratory, California Institute of Technology under contract with the National Aeronautics and Space Administration.

1. The antenna structural response due to gravity loading is linear.
2. The elevation-rigging angle (maximum gain) of the antenna can be accurately inferred from total power radiometry (TPR) efficiency measurements.
3. The antenna response to gravity loading is symmetric relative to the antenna elevation-rigging angle.

The derivation is based on computing two loading vectors Fig.2 of the total antenna effective deformation in the Y- and Z- axis directions [3]. The loading vector Y represents the total antenna deformation when the antenna elevation angle is 0-degrees, and the vector Z represents its total deformation at 90-degrees. The antenna deformations was computed at 5-degree increments in elevation and then ray traced to the DFP position to compute the displacements of the 16 actuators and thus derive its look-up table.

ANTENNA GRAVITY DEFORMATION DERIVATION

Physical reasoning shows that an antenna that is perfectly symmetrical in construction and weight distribution about the *XZ* and *YZ* planes, Fig.2, will deform in a symmetrical but conjugate way due to gravity. It is the deviation from this perfect symmetry in the antenna structure that requires sampling of the antenna deformation below and above the rigging angle (the angle of maximum antenna gain, typically around 45-degrees). Three angles are the minimum number of observations needed to derive an analytical model for the gravity deformation of an antenna. Due to the common deviation of antenna's structure from perfect symmetry, it is usually required that the full range of the elevation motion of the antenna be sampled including angles below and above the rigging angle. In the experimental antenna gravity deformation derived here, a perfect antenna structural symmetry was assumed. Thus, by using the MAHST and observing geostationary satellites, the highest elevation angle for observation that could be obtained was 47-degrees. In general, antenna deformation maps can be obtained at angles above the rigging angle by using other RF metrology techniques like phase retrieval or VLBI (Very Long Baseline Interferometry) holographic techniques. Dimensional metrologies like theodolite and laser tracker are other possibilities.

The analytical model used here is based on two loading vectors and an initial condition vector that encompassed the three unknowns for each node of the antenna surface description [3]. The positions of the nodes were coincidence with the holography resolution cell coordinate rather then based on finite element model (FEM). By choosing large number of approximately 10,000 cells (order of magnitude larger than the number of FEM nodes) no compromise was introduced. The model was applied to the antenna residual surface error deviation from the best-fit paraboloid [2]. Equation (1) represent the gravity deformation model used for each node of the antenna surface.

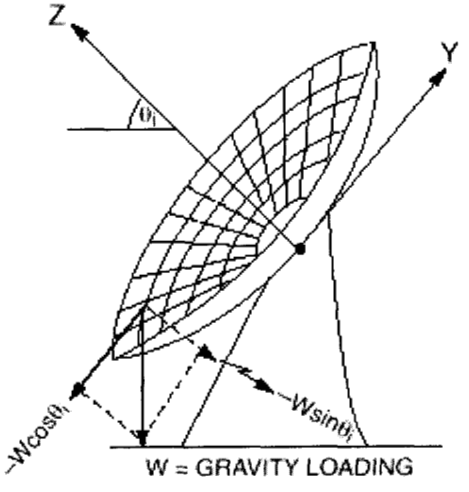

Fig. 2 Gravity Loading Components at Antenna Node

$$\varepsilon_{i,k}(el) = \varepsilon_{i,k}(el_m) + \rho^{z}_{i,k}[\sin(el_m) - \sin(el)] + \rho^{y}_{i,k}[\cos(el_m) - \cos(el)] \quad (1)$$

Where:

$\varepsilon_{i,k}(el)$: Residual antenna deformation at any elevation angle (*el*) at node *i,k*

el: Elevation angle

el_m: Elevation rigging angle

$\rho^{z}_{i,k}$: Loading vector in the Z-axis direction (see Fig.2) for node *i,k*

$\rho^{y}_{i,k}$: Loading vector in the *Y*-axis direction (see Fig.2) for node *i,k*

The gravity loading model applied to approximately 10,000 nodes (*i*=*k*=100) for the 70-meter antenna which has 1272 panels and 5,000 adjustment screws. When the number of deformation maps is limited to three angles (el_1, el_2, *and* el_m), the coefficients for the above equation can be solved in closed form:

$$\rho^{y}_{i,k} = \frac{[\sin(el_m) - \sin(el_1)]\Delta\varepsilon_{i,k}(el_m - el_2) - [\sin(el_m) - \sin(el_2)]\Delta\varepsilon_{i,k}(el_m - el_1)}{[\sin(el_m) - \sin(el_2)][\cos(el_m) - \cos(el_1)] - [\cos(el_m) - \cos(el_2)][\sin(el_m) - \sin(el_1)]} \quad (2)$$

$$\rho^{z}_{i,k} = -\frac{\Delta\varepsilon_{i,k}(el_m - el_2)}{\sin(el_m) - \sin(el_2)} - \rho^{y}_{i,k}\frac{\cos(el_m) - \cos(el_2)}{\sin(el_m) - \sin(el_2)} \quad (3)$$

Where:

el_1, el_2, el_m: The three elevation angles for the holographic measurements

$\Delta\varepsilon_{i,k}(el_m - el_i)$: The residual error difference at node i,k between elevation el_m and el_i

When more than three elevation angles are available, a least squares fit approach should be employed to derive the coefficients in equation (1).

The final derivation of the antenna deformation Fig.3 and Fig.4, was computed via (1) and assuming perfect conjugate structural symmetry with respect to the antenna rigging angle which was measured to be around 42-degrees.

From the surface distortion maps, ray optics was used to determine the theoretical shape of the DFP that will exactly phase compensate the distortions.

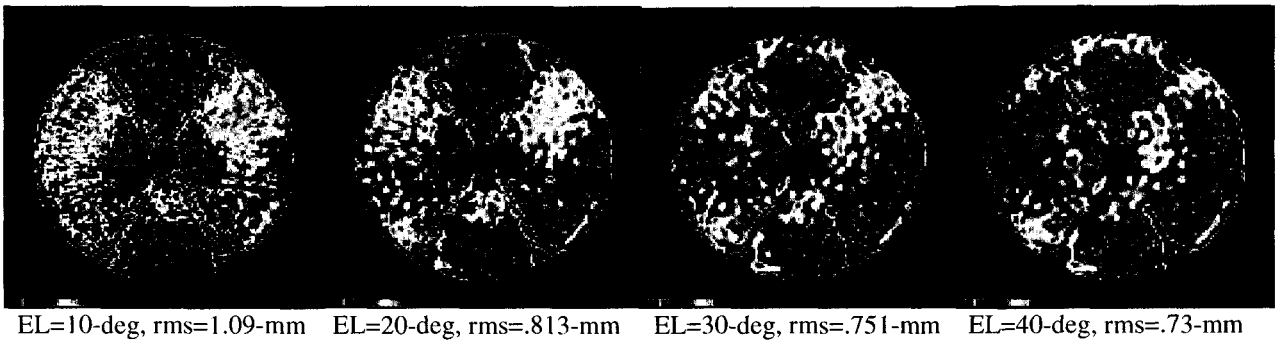

EL=10-deg, rms=1.09-mm EL=20-deg, rms=.813-mm EL=30-deg, rms=.751-mm EL=40-deg, rms=.73-mm

Fig.3 DSS-14 surface Deformation

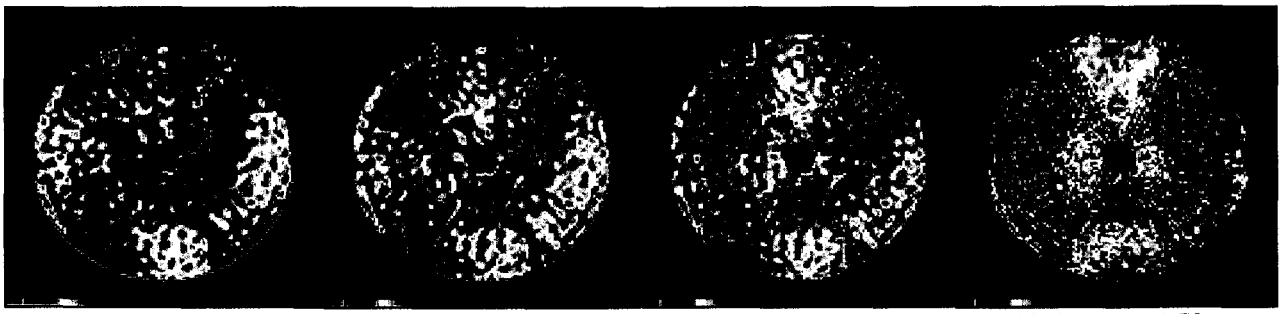

EL=50-deg, rms=.751-mm EL=50-deg, rms=.810-mm EL=70-deg, rms=1.09-mm EL=80-deg, rms=1.72-mm

Fig.4 DSS-14 surface Deformation

From the theoretical shape and a NASTRAN mechanical model of the DFP, the actuator positions that generate a surface that provides the best RMS fit to the theoretical model are selected. Using the actuator positions and the NASTRAN model provides an accurate description of the actual mirror shape. The above process was repeated at 5-degrees increment in elevation to derive 17 sets of the 16-actuator displacements, which were then entered into the antenna data acquisition computer controller. Testing of the applied DFP vectors was then measured and iteratively corrected and improved using the MAHST at 12.7-degrees elevation. Hence, an open loop calibration of the DFP was obtained. Fig.5 shows the gain improvement measured at DSS-14 at 32-GHz by using the DFP. The data was measured by tracking natural radio sources and obtaining antenna-temperature using total power radiometry (TPR).

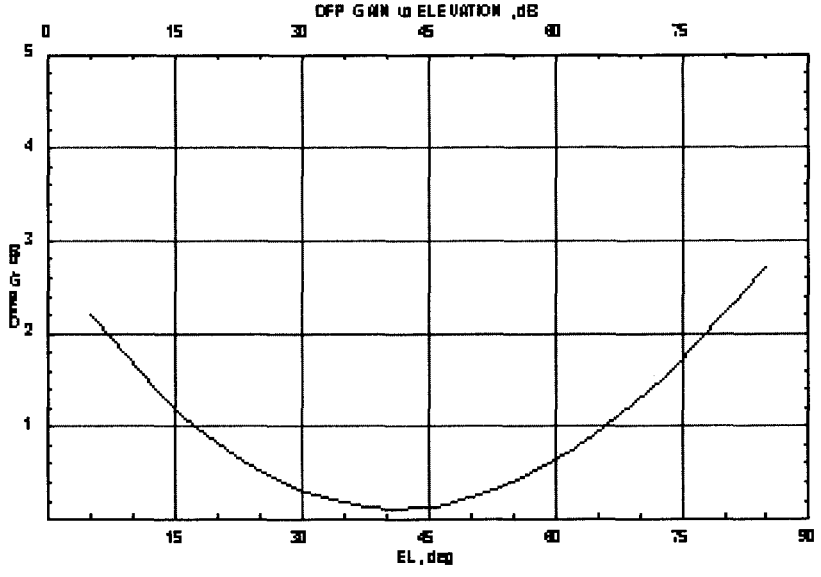

Fig.5 Gain Improvement of DSS-14 at 32-GHz as a Function of Elevation Resulting from DFP Compensation

REFERENCES

[1] R. Bruno, W. Imbriale, M. Moore and S. Stewart, "Implementation of a gravity compensation mirror on a large aperture antenna", *AIAA Multidisciplinary Analysis and Optimization*, Bellevue, WA, Sept. 1996.

[2] D.J. Rochblatt and B.L. Seidel, "Microwave Antenna Holography", *IEEE Trans. Microwave Theory and Techniques*, Special Issue on Microwaves in Space. Vol. 40, NO. 6, pp.1294-1300, June 1992.

[3] R. Levy, "*Structural Engineering of Microwave Antennas*", IEEE Antenna & Propagation Society, IEEE Press, 1996